DNA Repair 31 (2015) 19–28

Contents lists available at ScienceDirect

DNA Repair

journal homepage: www.elsevier.com/locate/dnarepair

Inhibition of the ERCC1–XPF structure-specific endonuclease to overcome cancer chemoresistance

Ewan M. McNeil[a,1,2], Katy R. Astell[a,1], Ann-Marie Ritchie[a], Steven Shave[b], Douglas R. Houston[b], Preeti Bakrania[c], Hayley M. Jones[c], Puneet Khurana[c], Claire Wallace[c], Tim Chapman[c], Martin A. Wear[b], Malcolm D. Walkinshaw[b], Barbara Saxty[c], David W. Melton[a,*]

[a] MRC Institute of Genetics and Molecular Medicine, University of Edinburgh, MRC Human Genetics Unit, Western General Hospital, Crewe Road, Edinburgh EH4 2XU, UK
[b] Centre for Translational and Chemical Biology, School of Biological Sciences, University of Edinburgh, Michael Swann Building, The King's Buildings, Mayfield Road, Edinburgh EH9 3JR, UK
[c] Centre for Therapeutics Discovery, MRC Technology, 1-3 Burtonhole Lane, Mill Hill, London NW7 1AD, UK

ARTICLE INFO

Article history:
Received 19 February 2015
Received in revised form 7 April 2015
Accepted 10 April 2015
Available online 22 April 2015

Keywords:
Nucleotide Excision Repair
Interstrand Crosslink Repair
DNA repair inhibitor
ERCC1–XPF
FANCQ
Melanoma
Ovarian cancer

ABSTRACT

ERCC1–XPF is a structure-specific endonuclease that is required for the repair of DNA lesions, generated by the widely used platinum-containing cancer chemotherapeutics such as cisplatin, through the Nucleotide Excision Repair and Interstrand Crosslink Repair pathways. Based on mouse xenograft experiments, where ERCC1-deficient melanomas were cured by cisplatin therapy, we proposed that inhibition of ERCC1–XPF could enhance the effectiveness of platinum-based chemotherapy. Here we report the identification and properties of inhibitors against two key targets on ERCC1–XPF. By targeting the ERCC1–XPF interaction domain we proposed that inhibition would disrupt the ERCC1–XPF heterodimer resulting in destabilisation of both proteins. Using *in silico* screening, we identified an inhibitor that bound to ERCC1–XPF in a biophysical assay, reduced the level of ERCC1–XPF complexes in ovarian cancer cells, inhibited Nucleotide Excision Repair and sensitised melanoma cells to cisplatin. We also utilised high throughput and *in silico* screening to identify the first reported inhibitors of the other key target, the XPF endonuclease domain. We demonstrate that two of these compounds display specificity *in vitro* for ERCC1–XPF over two other endonucleases, bind to ERCC1–XPF, inhibit Nucleotide Excision Repair in two independent assays and specifically sensitise Nucleotide Excision Repair-proficient, but not Nucleotide Excision Repair-deficient human and mouse cells to cisplatin.

1. Introduction

Either alone or in combination with other drugs the platinum-containing compounds, cisplatin, carboplatin and oxaliplatin, are the current mainstays of systemic therapy for many of the commonest cancer types: small cell and non-small cell lung cancer, aerodigestive, lower gastrointestinal, gynaecologic and genitourinary malignancies. In addition, they are important treatments in sub-sets of patients with breast cancer, non-Hodgkin's lymphoma and childhood malignancies. Although novel molecular targeted therapies are often incorporated into modern treatment algorithms, the mainstay of systemic treatment for the majority of patients is likely to continue to be cytotoxic chemotherapy for the foreseeable future.

For instance, ovarian cancer is the 5th most common cause of female cancer and the 4th most common cause of female cancer death in the UK, with 7116 new cases in 2011 and 4271 deaths in 2012 [1]. 75% of patients present with stage III or IV disease and, although 70–80% initially respond to surgery and platinum-based chemotherapy, in the vast majority platinum-resistant disease ultimately arises and subsequent survival is short. The ability to enhance platinum sensitivity would be a huge advantage, both in terms of increasing the efficacy of first line chemotherapy and also in terms of inducing further remissions in the setting of relapsed disease.

* Corresponding author. Tel.: +44 1314678449; fax: +44 1314678450.
E-mail address: David.Melton@ed.ac.uk (D.W. Melton).
[1] These authors contributed equally to this work.
[2] Present address: MRC Protein Phosphorylation Unit, College of Life Sciences, University of Dundee, Dundee DD1 5EH, UK.

http://dx.doi.org/10.1016/j.dnarep.2015.04.002
1568-7864/

Over the last 30 years the global incidence of melanoma has increased faster than any other form of cancer. It is now the second most common cancer amongst young adults in the UK [1]. Global incidence in 2009 was 134,000, and is predicted to increase to 165,000 by 2016. Early surgical removal of primary tumours is an effective treatment, but chemotherapeutics such as cisplatin are ineffective (5 year survival with the standard chemotherapeutic for melanoma, dacarbazine, is <15%). Although BRAF inhibitors, immunotherapies, and new combination therapies offer exciting prospects for improved survival, it is already clear that the development of resistance is a major problem and that there remains a need for additional effective melanoma therapy [2].

Platinum based chemotherapeutics, such as cisplatin, result in several forms of DNA damage. Bulky lesions and intrastrand crosslinks are removed by Nucleotide Excision Repair (NER). Interstrand crosslinks (ICLs), which are more toxic and so more effective therapeutically, are removed by Interstrand Crosslink Repair (ICR) utilising a combination of endonucleolytic cleavage, homologous recombination and translesion synthesis.

The ERCC1–XPF structure-specific DNA repair endonuclease is involved in the removal of platinum-DNA adducts. Data from a number of studies suggest that it is a promising target in melanoma, ovarian, lung and a range of other cancers [3]. ERCC1–XPF is essential for NER and is also involved in the endonucleolytic cleavage step in ICR. In tumours, such as non-small cell lung carcinoma [4–6], squamous cell carcinoma [7,8] and ovarian cancer [9], high ERCC1 expression has been linked in some studies with poor response to chemotherapy. In contrast, testicular cancers show low ERCC1 expression and can be effectively cured with cisplatin [10]. Furthermore, depletion of ERCC1–XPF with siRNA increases sensitivity to cisplatin in ovarian [11], non-small cell lung [12] and breast cancer [13] cell lines. Melanoma cells deficient in ERCC1 were 10-fold more sensitive to cisplatin than isogenic ERCC1-proficient cells and, using a mouse xenograft model, we showed that ERCC1-deficient melanoma can be cured by cisplatin therapy [14]. These observations led us to conclude that inhibition of ERCC1–XPF could be therapeutically advantageous in the treatment of cancers with chemotherapy [3].

ERCC1 is a 297 amino acid protein with a central domain which interacts with both DNA and the XPA protein [15,16], and a helix-hairpin-helix (HhH_2) domain essential for heterodimerization with XPF [15,17,18]. XPF (FANCQ) protein, at 916 amino acids, comprises of helicase-like [19–21], nuclease [22], and helix–hairpin–helix (HhH_2) domains [15,17,18]. The three most attractive targets on the ERCC1–XPF complex are the XPA-binding domain required for recruitment to the NER complex, the ERCC1–XPF heterodimerization domain required for stability, and the XPF endonuclease domain which is required for all known roles of ERCC1–XPF [3].

Despite widespread interest in ERCC1–XPF as a target, specific inhibitors have remained elusive. Interaction of the non-specific PK-C inhibitor, UCN-01, with ERCC1 Tyr residues within the ERCC1/XPA interaction site was reported to attenuate recruitment of ERCC1 to NER [23,24]. A synthetic peptide inhibitor of the ERCC1/XPA interaction was also designed that mimicked the interacting XPA region [16]. Small molecule inhibitors for the ERCC1/XPA interaction with activity against lung and colorectal cancer cell lines were then reported [24,25]. More recently an *in silico* drug screen has yielded inhibitors of the ERCC1–XPF interaction domain that, at very high concentration, can apparently disrupt ERCC1–XPF complex stability in cell lysates [26]. However, the potency and specificity of these inhibitors requires much improvement.

Here we design and deploy assays to identify small molecule interaction and active site inhibitors of the ERCC1–XPF structure-specific endonuclease and characterise their activity and specificity in *in vitro* assays and in cancer cells.

2. Materials and methods

2.1. Expression and purification of recombinant ERCC1–XPF proteins

Synthetic DNA sequences encoding human ERCC1 codons 96–297 (ΔERCC1) and XPF codons 667–916 (ΔXPF), codon-optimised for *E. coli* expression (GeneArt, Life Technologies Ltd., Paisley, UK), were cloned as BamHI–EcoRI fragments into separate pET-28a Kan^R expression vectors with N-terminal His-tags (Novagen, Merck Ltd., Nottingham, UK). Expression was in BL21 Star (DE3) *E. coli*. Details of the methods used to express and purify ΔERCC1–ΔXPF and separate ΔERCC1 and ΔXPF proteins are given in Supplementary Materials and Methods. A near full-length His-tagged version of human ERCC1–XPF (ERCC1 1–297, XPF 12–916) was also expressed from plasmid ERCC41 [27] and purified as described [28].

2.2. In silico *screens*

Searches for ERCC1–XPF interaction inhibitors and inhibitors of the active site of the XPF endonuclease domain were carried out as described in Supplementary Materials and Methods. First, our entire virtual library (>10^6 compounds) was screened using a fast docking code to elucidate a pharmacophore. This was then used to prioritise promising molecules for a second round of more accurate and computationally more expensive docking processes.

2.3. BIAcore SPR analysis

Kinetics of ΔERCC1 and ΔXPF interaction and screening for ERCC1–XPF interaction inhibitors were performed using the method developed by Wear et al. [29]. Details are given in Supplementary Materials and Methods.

2.4. Thermal denaturation assay

Details of the thermal denaturation assay to detect interaction of compounds with ΔERCC1–ΔXPF, by a change in the transition melting temperature of the protein, are given in Supplementary Materials and Methods.

2.5. In vitro *ERCC1–XPF endonuclease assay*

Details of the *in vitro* ERCC1–XPF endonuclease assay and the method to visualise cleavage products are given in Supplementary Materials and Methods.

2.6. In vitro *DNase I and FEN1 assays*

Details are given in Supplementary Materials and Methods.

2.7. Proximity ligation assay

Details of the PLA assay are given in Supplementary Materials and Methods.

2.8. Cell culture toxicity and cisplatin enhancement assays

Compound screening on A375 human melanoma cells was carried out as described in Supplementary Materials and Methods.

2.9. NER assays

Details of the transfection-based assay developed to monitor inhibition of NER in A375 melanoma cells and of the ELISA assay

to monitor repair of cyclobutane pyrimidine dimers are given in Supplementary Materials and Methods.

2.10. Determination of ERCC1 and XPF protein levels in cultured cells

Western blotting was performed as described [14]. Protein extraction and antibody details are given in Supplementary Materials and Methods.

3. Results

3.1. Expression of recombinant ERCC1–XPF proteins

In order to develop an *in vitro* endonuclease assay to monitor inhibition of ERCC1–XPF, it was first necessary to express and purify recombinant ERCC1–XPF proteins. The domain structure of the human ERCC1 and XPF proteins is shown in Fig. 1A. N-terminal His-tagged truncated versions of ERCC1 (residues 96–297, containing the central and HhH_2 domains) and XPF (residues 667–916, containing the endonuclease and HhH_2 domains) were constructed to express ΔERCC1–ΔXPF in *E. coli*. This truncation has previously been shown to have activity in an ERCC1–XPF endonuclease assay [15]. For comparison, a plasmid expressing a full-length His-tagged version of ERCC1–XPF was also used [27]. After induction and purification, ΔERCC1–ΔXPF protein with a size determined by gel filtration chromatography that matched the predicted M_r of 57.72 kDa, at >95% purity and with a yield of ~10 mg/l of culture was obtained (Fig. 1B and C). In comparison, full-length ERCC1–XPF protein, with a size by gel filtration chromatography that matched the predicted M_r of 151 kDa, at >90% purity, but with a yield of only ~50 μg/l of culture was obtained (Fig. 1B). Similar low yields of full-length ERCC1–XPF from the same plasmid have been reported previously [28].

3.2. Validation of in vitro ERCC1–XPF endonuclease assay for ΔERCC1–ΔXPF protein

An *in vitro* ERCC1–XPF endonuclease assay suitable for high throughput screening was established using the standard stem-loop DNA substrate originally used in a radiolabelled assay [15,30], but modified to incorporate a 5′ fluorescein label (6-FAM) and a 3′ Black Hole Quencher (BHQ-1). Upon ERCC1–XPF cleavage, a 10 nt 5′ FAM-labelled product is released resulting in a fluorescent signal (Supplementary Fig. 1A). An equivalent assay has been described previously [28]. Under standard reaction conditions we estimated that the full length ERCC1–XPF protein was 15-fold more active than the truncated form (Supplementary Fig. 1B and C). A similar difference between this truncation and full-length ERCC1–XPF has been reported previously [15]. Importantly, visualisation of substrate products from both ERCC1–XPF and ΔERCC1–ΔXPF reactions (Fig. 1D) showed the expected 10 nt product resulting from cleavage 2 nt upstream of the ds- to ss-DNA junction [15,28]. Although the increased activity was desirable, given the very low yields of purified ERCC1–XPF, the ΔERCC1–ΔXPF protein with the characteristic structure-specific endonuclease activity of ERCC1–XPF was used for all high throughput screening and inhibitor studies described here.

To demonstrate compound inhibition of this assay, we used the non-specific nuclease inhibitor aurintricarboxylic acid (ATA), which inhibited ΔERCC1–ΔXPF with an IC50 of 0.81 μM (Supplementary Fig. 2A). In agreement with literature, ATA also inhibited

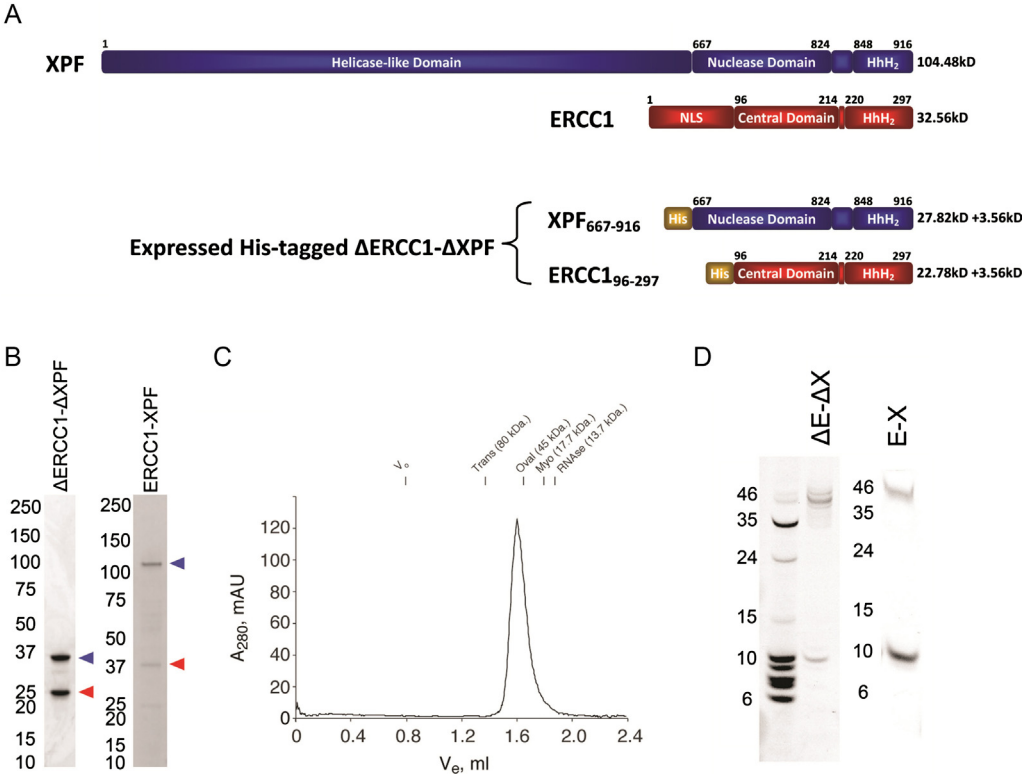

Fig. 1. Expression of recombinant ERCC1–XPF proteins for structure-specific endonuclease assay. (A) Schematic showing the domain architecture and M_r of full length ERCC1 and XPF subunits, and of the expressed truncated ΔERCC1–ΔXPF protein, with the M_r of the N-terminal His tags also indicated. (B) Gel showing purified recombinant ΔERCC1–ΔXPF and ERCC1–XPF proteins. Arrowheads indicate ERCC1 and XPF proteins. (C) Chromatograph from a Superdex-200 3.2/30 PC run showing final purity of ΔERCC1–ΔXPF complex. Elution positions of molecular weight markers are indicated. Apparent M_r of ΔERCC1–ΔXPF complex is ~57 kDa. (D) Visualisation of 6-FAM-labelled reaction products for full length and ΔERCC1–ΔXPF proteins following endonuclease assay and denaturing polyacrylamide gel electrophoresis. 6-FAM-labelled oligonucleotide markers are also shown. Note that the main cleavage product for both full-length and ΔERCC1–ΔXPF is the expected 10 nt fragment.

a bovine DNase I assay with an IC50 of 6.6 μM (Supplementary Fig. 2B) [31,32] and a recombinant human Flap endonuclease 1 (FEN1) assay with an IC50 of 1.8 μM (Supplementary Fig. 2C) [33]. FEN1, a related endonuclease to ERCC1–XPF, but with a different structure-specificity, was chosen to provide a strong test of the specificity of our ERCC1–XPF inhibitors.

3.3. Identification of ERCC1–XPF interaction inhibitors

3.3.1. In silico *screen*

We sought to identify inhibitors of the interaction between ERCC1 and XPF helix–hairpin–helix (HhH_2) domains, thereby disrupting heterodimer stability and so enhancing sensitivity to platinum-based chemotherapeutics. Previously we identified the ERCC1 Phe293 pocket on XPF (Fig. 2A) as a prospective target [3]. From the ERCC1–XPF HhH_2 crystal structure (PDB 2A1J) [15] we identified two further interaction sites on XPF where ERCC1 Ile264 and Cys238 residues make contact. We then performed *in silico* screens targeting the Phe293 or Ile264 pockets, and pairwise pocket combinations. The 29 top-ranked compounds (Supplementary Table 1) were investigated for activity *in vitro*. The ERCC1–XPF endonuclease assay was considered inappropriate for interaction inhibitors since it uses a preformed complex which, it was reasoned, would be much harder for an interaction inhibitor to disrupt than prevent from forming. Instead, evidence of physical binding to the XPF target was sought.

3.3.2. Validation by BIAcore SPR analysis

We first expressed recombinant ΔERCC1 and ΔXPF separately and determined the kinetic parameters for their interaction. The affinity of the ΔERCC1–ΔXPF interaction was 4.6 nM (Fig. 2B), with apparent on- and off-rate constants indicating that complex recognition is rapid and that stable complex formation occurs with a long half-life of 120–150 s. This suggests interaction is specific, tight and that once complex formation occurs in cells, it is unlikely to dissociate in an unregulated manner. To demonstrate activity of ERCC1–XPF interaction inhibitors, compounds were screened at 100 μM against ΔXPF protein linked to the SPR surface. Interaction with XPF was determined relative to the control surface with responses corrected for molecular weight. If interaction was observed, a concentration series was then performed. Of the compounds from the *in silico* screens purchased for validation, 4 bound specifically to ΔXPF. Steady-state analysis gave Kd values of 17.8, 275, 537 and 200 μM for E-X PPI1 to 4 (ERCC1–XPF protein–protein interaction inhibitors 1 to 4), respectively, with stoichiometric ratios for XPF binding of $n \sim 1{:}1$, 1:2, 1:2 and 1:3, respectively. The predicted binding pose for E-X PPI2, which targets the Phe293 & Cys238 pockets, is shown in Fig. 2C. Aurintricarboxylic acid (ATA) could not be used as a positive control as this bound irreversibly to ΔXPF at super-stoichiometric ratios ($n \sim 1{:}40$).

3.4. Activity of ERCC1–XPF interaction inhibitor E-X PPI2 in cancer cells

3.4.1. Inhibition of Nucleotide Excision Repair in melanoma cells

A transfection-based assay was established in A375 melanoma cells to measure NER of UV-damaged plasmid DNA. UV was chosen as the damaging agent over cisplatin because all UVC-induced lesions are substrates for NER, while other repair pathways are also involved in the repair of some platinated DNA lesions. Cells were incubated with compounds for 24 h and then co-transfected with a UV-irradiated or undamaged GFP-expressing plasmid, together with a luciferase-expressing control plasmid. The level of UV-irradiation used in the assay was first calibrated using NER-proficient A375 and NER-deficient XP12RO cells to ensure that any expression from the irradiated GFP plasmid was due to repair rather than expression from any non-damaged plasmid DNA (see Supplementary Fig. 3). 24 h after transfection the level of GFP and luciferase expression was measured and the GFP/luciferase ratio calculated. The luciferase signal provides a control for transfection efficiency and for any non-NER-related effects of the compounds. For each compound concentration, the effect of the compound on NER was determined by dividing the GFP/luciferase ratio for the

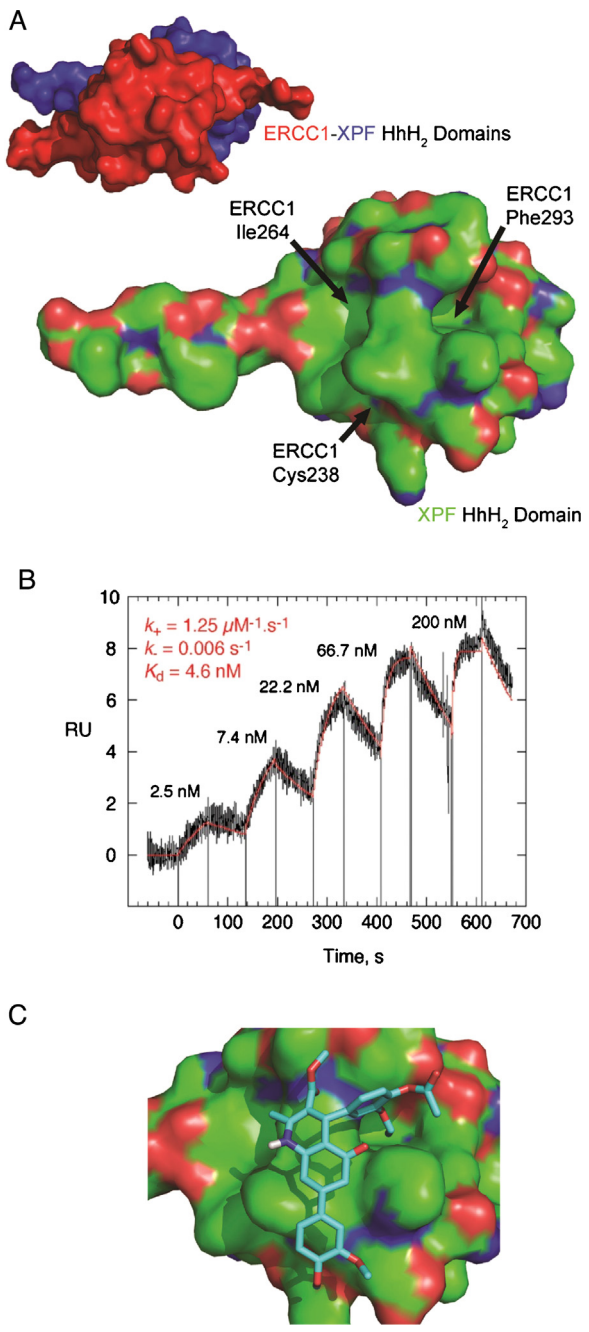

Fig. 2. *In silico* screening for ERCC1–XPF interaction inhibitors. (A) ERCC1–XPF HhH_2 heterodimerization complex (PDB Code 2A1J), with ERCC1 on top. Also shown is the heterodimerization surface of XPF (using the Connolly surface), identifying the binding pockets for ERCC1 residues Cys238, Ile264 and Phe293. (B) Heterodimerization of recombinant ΔERCC1 and ΔXPF proteins analysed using BIAcore T200 SPR. Reference corrected single cycle kinetic titration SPR binding curves, monitored on a surface of 276 RU of covalently stabilised ΔXPF, for the indicated concentrations of ΔERCC1. The apparent on- and off-rate constants were determined by globally fitting a 1:1 kinetic binding model with mass transport considerations to the sensorgrams. (C) Structure and binding pose of E-X PPI2 to the Phe293 and Cys238 pockets; docked affinity 52 μM, ligand efficiency 0.15.

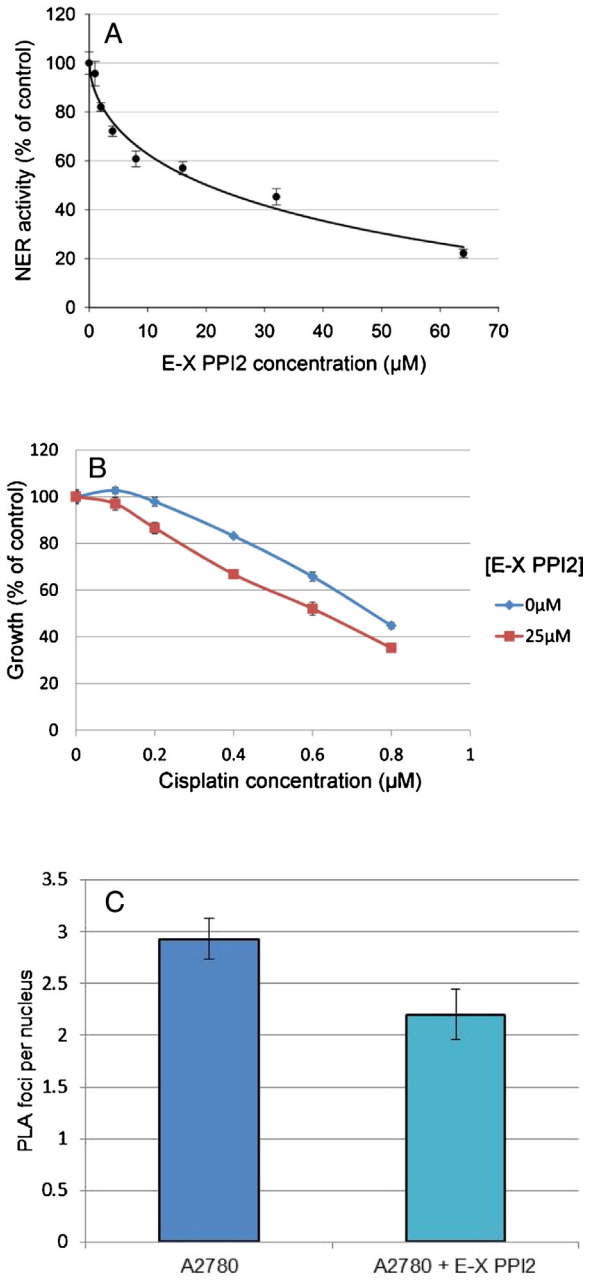

Fig. 3. Activity of ERCC1–XPF interaction inhibitor E-X PPI2 in cancer cells. (A) Inhibition of NER in the A375 human melanoma cell line. Values plotted are the mean NER activity (±SEM) from two independent experiments as a percentage of activity in control cells. IC50 20 μM. (B) Sensitisation of A375 melanoma cells to cisplatin. Standard 5-day SRB growth assay in 96-well plates showing enhanced sensitivity to cisplatin (1.3-fold) in the presence of 25 μM E-X PPI2. For each curve, growth is expressed as the percentage of the non-cisplatin-treated control. Values plotted are mean % growth (±SEM) from three independent experiments. (C) Reduction in ERCC1–XPF heterodimer levels in A2780 human ovarian cancer cells. *In situ* proximity ligation assay (PLA) with antibodies against ERCC1 and XPF on control A2780 cells and cells treated for 5 days with 75 μM E-X PPI2. >600 nuclei in 11 separate microscopic fields were scored for each condition and the mean number of PLA foci per nucleus (±SEM) is shown.

damaged GFP plasmid by the same ratio for the non-damaged GFP plasmid. This value was then divided by the equivalent value for control cultures without any compound and plotted as % NER activity against compound concentration to obtain the IC50. Only E-X PPI2 from the 4 interaction inhibitor compounds, with an IC50 of 20 μM, showed activity in the NER assay (Fig. 3A). This was the only interaction inhibitor that was investigated further.

3.4.2. *E-X PPI2 enhances melanoma cell sensitivity to cisplatin*

To further investigate ERCC1–XPF inhibitory activity in cell culture, we first determined the basic toxicity in A375 human melanoma cells in a growth assay. Then the ability of the compound, at concentrations less than the IC50, to sensitise the growth of melanoma cells to cisplatin was determined. While an ideal inhibitor would reduce the cisplatin IC50 by 10-fold as we observed for isogenic ERCC1-proficient and -deficient mouse melanoma cells [14], data using siRNA against ERCC1 or XPF show more modest 2–3-fold shifts in the cisplatin IC50 [12]. E-X PPI2 caused a small (1.3-fold) reduction in the cisplatin IC50 (Fig. 3B).

3.4.3. *Reduction in ERCC1–XPF heterodimer levels in ovarian cancer cells after E-X PPI2 treatment*

Heterodimerization is essential for ERCC1–XPF function and is believed to be required for the stability of both proteins. We used antibodies to ERCC1 and XPF in an *in situ* proximity ligation assay (PLA) to investigate whether E-X PPI2 could affect heterodimer levels. PLA signals (nuclear foci) are only generated if both proteins are in close contact. A2780 human ovarian cancer cells cultured for 5 days in the presence of 75 μM E-X PPI2 showed a significant 25% reduction in the number of nuclear PLA foci ($p = 0.026$, Fig. 3C and Supplementary Fig. 4A). A similar reduction in the level of ERCC1 and XPF proteins was seen by western blotting (Supplementary Fig. 4B) and we conclude that this interaction inhibitor is indeed able to affect ERCC1–XPF heterodimer levels.

3.5. *Identification of ERCC1–XPF active site inhibitors*

3.5.1. In silico *screen*

While no crystal structure is available for the human XPF endonuclease domain, a structure exists for an archaebacterial homologue (PDB 2BGW) [34] (Supplementary Fig. 5A). A PHYRE-generated homology model [35] of human XPF was produced from this structure and used in the screen (Supplementary Fig. 5B). The top 100 compounds from the final ranked list (described in Supplementary Materials and Methods) were purchased and investigated; 4 compounds showed reproducible activity in the *in vitro* ΔERCC1–ΔXPF assay. The predicted binding poses for two of these compounds, E-X AS1 (ERCC1–XPF active site inhibitor 1) and E-X AS2, are shown in Supplementary Fig. 5C and D.

3.5.2. *High throughput screen*

A high throughput screen was performed with compounds at 20 μM in the ΔERCC1–ΔXPF assay. To ensure consistency, an ATA inhibitor control was included on each plate and an assay $Z' > 0.4$ was maintained [36]. A low hit rate was observed: of 101,440 compounds screened from the MRC Technology diversity library, 541 gave activity 3-fold less than the standard deviation, and the number was further reduced to 384 for compounds additionally showing <70% residual activity. Compounds were then subjected to a full IC50 determination, 87 resulted in inhibition with 49 showing an IC50 <200 μM and Hill slope <2. Following structural triage and removal of frequent hit compounds, 30 were re-screened in the ΔERCC1–ΔXPF assay, with 24 compounds reconfirming. To exclude non-specific nuclease inhibitors, the remaining compounds were screened for activity against DNase I and one was eliminated. Aggregating compounds were further excluded by testing inhibition in the presence of 10 times the normal concentration of enzyme under linear reaction conditions [37]. Two compounds with more than a ten-fold shift in the IC50 measured were excluded from further analysis.

3.5.3. *Hit confirmation by thermal denaturation assay*

The lack of a positive control for BIAcore SPR analysis meant that instead we used a thermal denaturation assay for confirmation

Table 1
Properties of FEN1 inhibitor analogues in endonuclease assays. (A) Compound ID. (B) Compound IC50 value in ΔERCC1–ΔXPF assay. (C) IC50 value in DNase I assay. (D) IC50 value in FEN1 assay. All IC50 values are the means from two separate determinations.

(A) ID	(B) ERCC1 IC50 (μM)	(C) DNase I IC50 (μM)	(D) FEN1 IC50 (μM)
E-X AS5	29.7	NA	0.30
E-X AS5-1	1.5	NA	0.06
E-X AS5-2	1.8	NA	0.003
E-X AS5-3	3.9	NA	0.01
E-X AS5-4	6.4	NA	2.11

NA, no activity.

of active site inhibitor hits. Using 5 μM ΔERCC1–ΔXPF protein with the stem-loop substrate as a positive control, the transition melting temperature (Tm) of ΔERCC1–ΔXPF increased in a concentration-dependent manner by up to 3 °C. At this maximum level, the substrate was present at 5 μM, consistent with predicted 1:1 stoichiometric binding (Supplementary Fig. 6). Two of the four compounds from the *in silico* screen, E-X AS1 and E-X AS2, and 7 of the remaining 21 compounds from the high throughput screen, E-X AS3 to 9, gave an increase in transition melting temperature and so provided evidence of binding to target (Supplementary Table 2).

3.5.4. *Specificity in* vitro *endonuclease assays*

The IC50 values for the remaining 9 active site inhibitor hits were determined in the ΔERCC1–ΔXPF endonuclease assay. In addition, compounds were screened against DNase I and FEN1 to investigate their specificity (Supplementary Table 2). The 2 active site inhibitors from the *in silico* screen (E-X AS1 and 2) showed good activity against ΔERCC1–ΔXPF, with no activity against the other endonucleases. E-X AS3 and 4, from the high throughput screen, showed good activity against ΔERCC1–ΔXPF, but were also active against FEN1. Although E-X AS5 was active against ERCC1–XPF, it was 100-times more active against FEN1. The structure of E-X AS5 is closely related to that of a previously described hit from a FEN1 inhibitor screen [38]. The remaining inhibitors from the high throughput screen, E-X AS6 to 9 were active against ΔERCC1–ΔXPF, but inactive against DNase I and FEN1. The structures of all the compounds in Supplementary Table 2 are shown in Supplementary Fig. 7.

3.6. *Structure activity relationships of inhibitors active against both ERCC1–XPF and FEN1*

Given the structural similarity of compound E-X AS5 to known FEN1 inhibitors, four analogues were synthesised and tested to compare their structure activity relationships against ΔERCC1–ΔXPF and FEN1 (Table 1 and Supplementary Fig. 7). Compounds E-X AS5-1 to E-X AS5-3 are described as highly potent FEN1 inhibitors [38] and it was found that these structural modifications led to gains in potency against ΔERCC1–ΔXPF compared with the initial hit E-X AS5, although they remained highly selective for FEN1. More encouragingly, E-X AS5-4 showed 4-fold increased activity against ΔERCC1–ΔXPF and 7-fold reduced activity against FEN1 compared with E-X AS5.

3.7. *Activity of ERCC1–XPF active site inhibitors E-X AS5-4 and E-X AS7 in melanoma cells*

Two of the active site inhibitors arising from the high throughput screen were selected for study of inhibitory activity in melanoma cells: E-X AS5-4 because it had a plausible mode of action through a metal-mediated interaction at the endonuclease active site and it also showed an encouraging improvement in specificity for ERCC1–XPF over FEN1 compared to the original hit, E-X AS5; and E-X AS7, which showed strong specificity for ERCC1–XPF in the biochemical assay and provided a metal-binding motif on an alternative molecular scaffold to E-X AS5, that was amenable to modification to remove unwanted features.

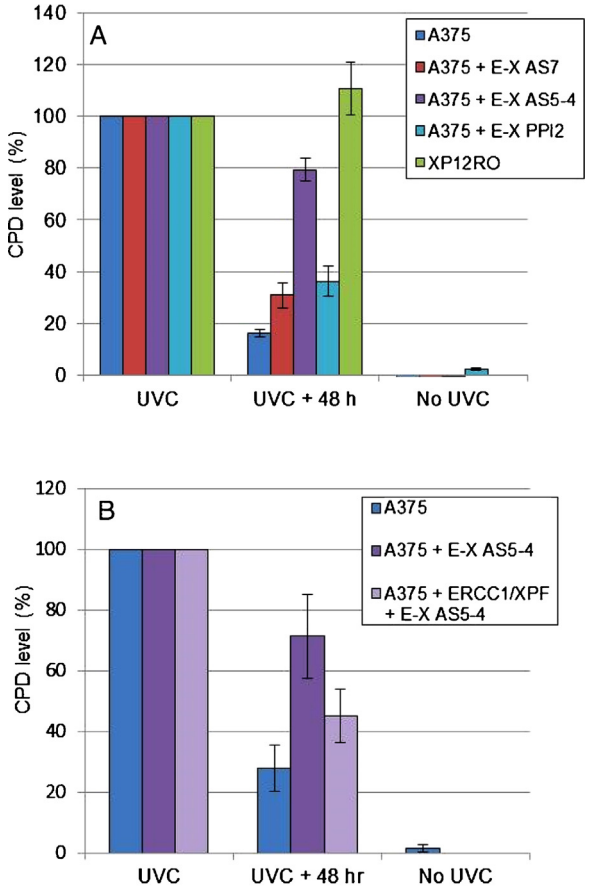

Fig. 4. Inhibition of cyclobutane pyrimidine dimer removal by active site inhibitor E-X AS5-4 that can be partially overcome by ERCC1–XPF overexpression. (A) Human NER-proficient (A375) and -deficient (XP12RO) cells were irradiated with 15 Jm^{-2} UVC and the level of CPDs in genomic DNA was determined by ELISA assay 2 h after irradiation and again after 48 h to allow time for repair. During this time A375 cells were also incubated in the presence of 32 μM E-X AS5-4, 4 μM E-X AS7, or 75 μM E-X PPI2 to determine their ability to inhibit repair of CPDs. The level of CPDs in non-irradiated cells was also determined. For each condition the level of CPDs (±SEM from 3 or more independent experiments) is shown as a percentage of the level 2 h after irradiation. (B) A375 cells were UV-irradiated and treated with 32 μM E-X AS5-4 for 48 h as in panel A. In addition, separate A375 cultures were also transiently co-transfected with ERCC1- and XPF-expressing plasmids 24 h before irradiation and treatment with 32 μM E-X AS5-4 for 48 h. For each condition the level of CPDs (±SEM from 3 independent experiments) is shown as a percentage of the level 2 h after irradiation.

3.7.1. *Inhibition of Nucleotide Excision Repair*

E-X AS5-4 (IC50 10 μM) and E-X AS7 (IC50 2 μM) both showed good activity in the transfection-based NER assay of UV-damaged plasmid DNA in A375 melanoma cells. We also investigated the activity of these active site inhibitors and the interaction inhibitor E-X PPI2 in an independent NER assay. All three compounds showed inhibition in an ELISA assay for the removal of UV-induced cyclobutane pyrimidine dimers (CPDs). 48 h after 15 Jm^{-2} of UVC, >80% of CPDs had been repaired in A375 melanoma cells, whereas no removal of CPDs had occurred in NER-deficient XP12RO cells (Fig. 4A). For A375 cells incubated with 32 μM E-X AS5-4, only 20% of the CPDs had been removed ($p = 0.0006$ compared to inhibitor-free cultures). For A375 cells incubated with 4 μM E-X AS7, the

inhibition of NER was lower but still significant, with twice the level of CPDs remaining compared to the non-treated control ($p = 0.048$). Similar inhibition was also observed when A375 cells were incubated with 75 μM E-X PPI2, although the result just failed to achieve conventional significance ($p = 0.057$).

Although all three compounds caused some slowing of the growth rate when A375 cells were treated for 5 days, flow cytometry showed that there were no substantial effects on the cell cycle profile or the levels of apoptosis (Supplementary Fig. 8A and B). In addition, western blotting showed no evidence for any reduction in levels of ERCC1 and XPF proteins after treatment with the two active site inhibitors, E-X AS5-4 and E-X AS7 (Supplementary Fig. 8C). We conclude that the ability of these three compounds to inhibit NER is most likely due to specific activity against ERCC1–XPF rather than to non-specific effects.

3.7.2. *Inhibition of NER can be partially overcome by overexpression of ERCC1–XPF*

If the strong inhibition of CPD removal by E-X AS5-4 is really due to a specific action against ERCC1–XPF, we reasoned that its action should be overcome by overexpressing the target. So, we transiently co-transfected A375 cells with plasmids expressing full-length human ERCC1 and XPF before repeating the ELISA assay for the removal of UV-induced CPDs in the presence of 32 μM E-X AS5-4. The extent of ERCC1–XPF overexpression achieved can be seen in Supplementary Fig. 9. In this experiment 74% of CPDs remained 48 h after UV irradiation in the presence of the inhibitor. ERCC1–XPF overexpression resulted in a significant reduction in CPDs remaining to 43% (Fig. 4B, $p = 0.04$), indicating that this inhibitor is indeed targeting ERCC1–XPF.

3.7.3. *Specificity of action of active site inhibitors*

We then investigated the specificity of action of E-X AS5-4 and E-X AS7 in a different way. If the ability of both compounds to enhance the sensitivity of NER-proficient A375 human melanoma cells to cisplatin is due to inhibition of ERCC1–XPF rather than to an off-target action, then no effect on the cisplatin sensitivity of NER-deficient cells should be observed. Since suitable immortalised human cells with complete deficiency in ERCC1 were not available, we used instead XP12RO, an immortalised NER-deficient cell line from a xeroderma pigmentosum complementation group A patient. We also used the PF20/PF24 mouse embryonic fibroblast cell line pair derived from ERCC1 knockout (PF24) and control (PF20) embryos. Based on IC50 values, XP12RO was 2.7 times more sensitive to cisplatin than A375, while PF24 was 5.6 times more sensitive than PF20. E-X AS5-4 enhanced the cisplatin sensitivity of A375 by 1.2-fold ($p = 0.05$) and of PF20 by 1.7-fold ($p = 0.016$), while having no effect on the cisplatin sensitivity of XP12RO ($p = 0.1$) and PF24 ($p = 0.39$) (Fig. 5A and B). E-X AS7 had a greater effect on the repair-proficient cell lines, enhancing cisplatin sensitivity of A375 by 1.6-fold ($p = 0.006$), and PF20 by 2.1-fold ($p = 0.002$), again with no effect on repair-deficient XP12RO ($p = 0.08$), and PF24 ($p = 0.53$) (Fig. 5C and D). Thus, both E-X AS5-4 and E-X AS7 showed the activity expected in cultured cells of a specific ERCC1–XPF inhibitor.

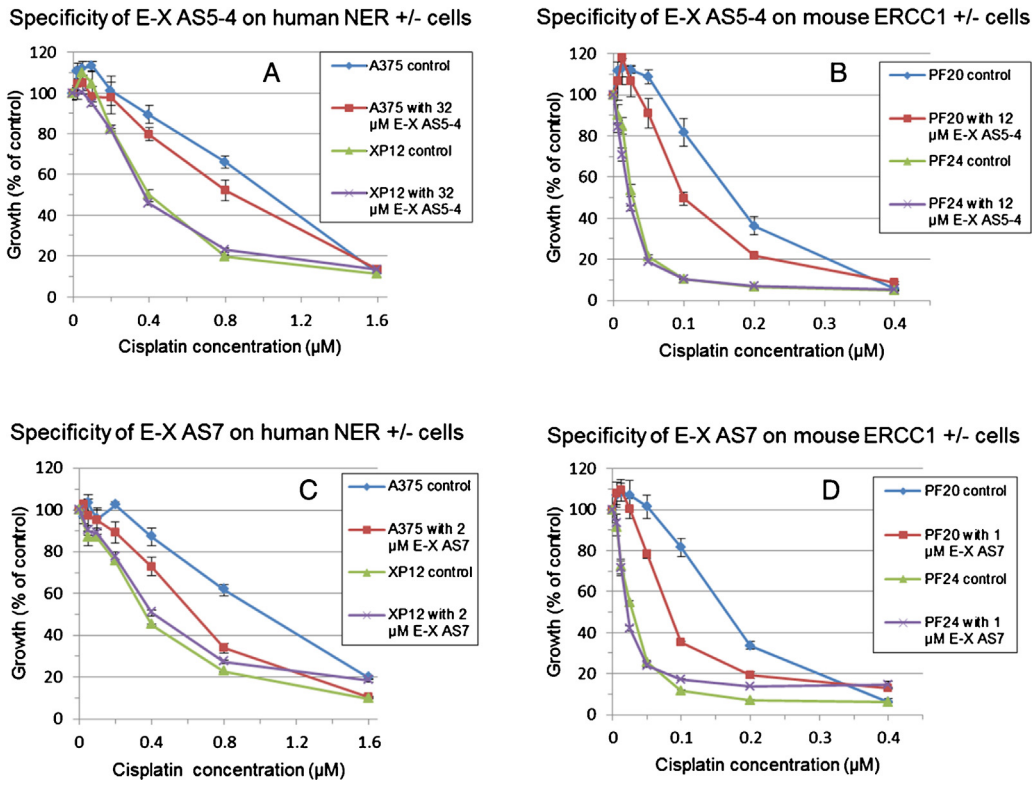

Fig. 5. Specificity of ERCC1–XPF active site inhibitors E-X AS5-4 and E-X AS7. Standard 5-day SRB growth assays in 96-well plates showing the effect on sensitivity to cisplatin of E-X AS5-4 and E-X AS7 in NER-proficient and -deficient human and mouse cells. For each curve, growth is expressed as the percentage of the non-cisplatin-treated control. Values plotted are mean % growth (±SEM) from two independent experiments. (A) Human NER-proficient (A375) and -deficient (XP12RO) cells in the presence and absence of 32 μM E-X AS5-4. Cisplatin IC50s: A375 control 1.04 μM, with E-X AS5-4 0.86 μM; XP12RO control 0.4 μM, with E-X AS5-4 0.39 μM. (B) Mouse ERCC1-proficient (PF20) and -deficient (PF24) cells in the presence and absence of 12 μM E-X AS5-4. Cisplatin IC50s: PF20 control 0.17 μM, with E-X AS5-4 0.1 μM; PF24 control 0.03 μM, with E-X AS5-4 0.028 μM. (C) Human NER-proficient (A375) and -deficient (XP12RO) cells in the presence and absence of 2 μM E-X AS7. Cisplatin IC50s: A375 control 1.04 μM, with E-X AS7 0.64 μM; XP12RO control 0.38 μM, with E-X AS7 0.4 μM. (C) Mouse ERCC1-proficient (PF20) and -deficient (PF24) cells in the presence and absence of 1 μM E-X AS7. Cisplatin IC50s: PF20 control 0.165 μM, with E-X AS7 0.08 μM; PF24 control 0.03 μM, with E-X AS7 0.026 μM.

4. Discussion

Our *in vitro* endonuclease assay for ERCC1–XPF activity was based around a truncated version of the heterodimer (ΔERCC1–ΔXPF), which was expressed at 200-fold higher levels than the full length protein. While both full-length and ΔERCC1–ΔXPF proteins were active in the endonuclease assay, the full length protein was approximately 15-fold more active. When recombinant protein production was performed in baculovirus, rather than the *E. coli* system used here, it was estimated that the same ΔERCC1–ΔXPF protein was 60-fold less active than the full-length form [15]. More recently, no activity was observed from a similar truncation (ERCC1 1–297, XPF 640–916) and it was suggested that activity from the ΔERCC1–ΔXPF protein could be due to contaminating non-specific nuclease activity [28]. In our assay, using the highly purified ΔERCC1–ΔXPF protein, we observed the expected ERCC1–XPF substrate cleavage specificity, 2 nt upstream of the ss- ds-DNA junction and we concluded that the ΔERCC1–ΔXPF protein does indeed retain the characteristic structure-specific endonuclease activity of ERCC1–XPF and so was suitable for our inhibitor studies.

An initial *in silico* screening approach for ERCC1–XPF inhibitors identified compounds that bound to the XPA-interacting pocket of ERCC1. One compound, NERI01 (AB-00026258), enhanced by 2-fold the sensitivity of a human colon cancer cell line to UV irradiation, but had a much weaker effect on cisplatin sensitivity [24,25]. Since effective disruption of this interaction would only inhibit ERCC1–XPF recruitment to NER complexes, we would expect it to be insufficient to fully sensitise cancer cells to platinum-based chemotherapy where ERCC1–XPF is recruited for Interstrand Crosslink Repair by an XPA-independent pathway [3]. We sought instead to discover inhibitors of the ERCC1–XPF interaction and XPF endonuclease domains, which are required for all known functions of ERCC1–XPF.

In order to discover inhibitors of the ERCC1–XPF interaction domain, we targeted the deep pocket on the interacting surface of XPF into which ERCC1 Phe293 fits and two adjacent shallower pockets for ERCC1 Ile264 and Cys238. Although our BIAcore SPR analysis indicated that the HhH_2 domain interaction between ERCC1 and XPF was likely too strong to be disrupted, inhibiting *de novo* complex formation was more realistic. We showed interaction of four of our screened putative interaction inhibitors with XPF, albeit with disassociation constants in the μM rather than nM range. As no suitable positive control was available, the total activity of the surface could not be determined so binding affinities and stoichiometries should be regarded as estimates. The complexity in the data meant that we could not use a standard 1:1 kinetic model. Instead, data were fitted to a 1:1 Langmuir steady-state model, but saturation response levels were lower than would be expected. This could be explained simply if the specific activity of the protein is lower than expected, which is a well-accepted caveat for SPR analysis. We controlled for non-specific compound binding by subtracting compound interaction with a surface lacking protein, and having a standard known promiscuous surface, HSA (human serum albumin), immobilised to the same equivalent activity level. We compared the binding effects to HSA and to the target surface and only took forward compounds with better binding or better predicted stoichiometry to the target. We have good evidence for compounds binding to target in a saturable manner, but lack of validation of the surface hampers our ability to conclude that it is target-specific and not just protein surface-specific.

Of the four putative interaction inhibitors, only E-X PPI2 was active in the inhibition of NER assay and it also showed some enhancement of cisplatin sensitivity in A375 human melanoma cells. Encouragingly however, and albeit at high concentration, E-X PPI2 treatment of human ovarian cancer cells resulted in significantly reduced levels of ERCC1–XPF heterodimers, suggesting that it was indeed able to inhibit the *de novo* complex formation that is considered essential for the stability of both proteins [39]. We acknowledge that it will be extremely difficult to effectively block ERCC1–XPF activity with this protein–protein interaction inhibitor approach. Inhibitors with much higher affinities than those currently available would be needed before there could be any therapeutic benefit.

Using a molecular dynamics *in silico* screening approach, Jordheim *et al.* have also described ERCC1–XPF interaction inhibitors [26]. One compound (F06, NSC 130813) caused a modest enhancement of sensitivity to cisplatin and mitomycin C (another interstrand crosslinker) in two cancer cell lines. Data from incubating cell extracts with high concentrations of FO6 (up to 500 μM), followed by immunoprecipitation, were interpreted to indicate that the compound can disrupt the interaction between the two proteins, but insufficient controls were shown to support this conclusion. Given the reported cytotoxicity of the FO6 compound and that a search of the PubChem database [40] reported activity in 51 of 368 bioassays against a range of different targets, it seems more likely that these actions are due to non-specific inhibitory activity, rather than the action of a specific ERCC1–XPF interaction inhibitor. More encouragingly, none of the compounds we identified (shown in Supplementary Fig. 7) appear as frequent hits in bioactivity screens in the PubChem database [40].

Our compounds and those identified by Jordheim et al. are targeted towards inhibiting the HhH_2 domain interaction between ERCC1 and XPF. *In vitro* mutagenesis on human ERCC1–XPF revealed the HhH_2 domain interaction to be essential, with deletion of 5 C-terminal residues being sufficient to abrogate dimerization (implicating ERCC1 Phe293 as an essential residue) [41,42]. However, the *in vivo* situation may be more complicated. While cells isolated from mice lacking ERCC1 are hypersensitive to UV-induced DNA damage [43], cells from mice lacking the 7 amino acids from the C-terminus of ERCC1 (including the equivalent residue to Phe293) may have some residual activity [44]. In addition, an extra protein–protein interaction between the nuclease domain of XPF and the central domain of ERCC1 has been proposed [3,15].

For XPF endonuclease domain inhibitors the challenge was to identify nuclease inhibitors with specificity for ERCC1–XPF. Two of the inhibitors arising from the high throughput screen, with good selectivity for ERCC1–XPF over DNaseI, and evidence of binding to target from a thermal denaturation assay, were selected for further study in cancer cells. E-X AS5 contains the *N*-hydroxy urea metal-binding motif found in previously described FEN1 inhibitors [38]. In its selected derivative, E-X AS5-4, a 4-fold potency gain against ERCC1–XPF coincided with 7-fold reduced activity against FEN1, suggesting that it may be possible to reverse the selectivity in favour of ERCC1–XPF inhibition. The hypothesis that these compounds are able to bind to ERCC1–XPF through interaction with a Mg^{2+} or Mn^{2+} ion at the endonuclease active site is supported by the fact that when the *N*-hydroxy motif is replaced by either *N*-H or *N*-methyl, thereby removing the potential for metal-binding, inhibitory activity was lost. The second compound selected, E-X AS7, displayed good selectivity against FEN1 and DNase I and also has potential to bind to the endonuclease site *via* a metal-based interaction through its catechol motif. However, it contains an undesirable hydrazone motif and showed relatively high toxicity in A375 cells.

Both E-X AS5-4 and E-X AS7 showed strong inhibition of NER in a UV-damaged plasmid-based transfection assay in melanoma cells and inhibition was confirmed in an independent ELISA assay for removal of UV-induced cyclobutane pyrimidine dimers. The CPD assay was also used to demonstrate that the action of the strongest active site inhibitor, E-X AS5-4, could be partially overcome by ERCC1–XPF overexpression, providing good evidence for target specificity. Further evidence for the target specificity of these

two active site inhibitors was provided by their ability to increase the cisplatin sensitivity of NER-proficient human and mouse cells, while having no effect on the paired NER-deficient cell lines.

While the attractions of the clinical application of an ERCC1–XPF inhibitor to enhance the effectiveness of the major class of current cancer chemotherapeutics are obvious, there are legitimate concerns about toxicity. It might be anticipated that an ERCC1–XPF inhibitor would show dose limiting toxicity. However, it is important to consider this in the context of inhibitors against other DNA repair proteins now in successful trials, such as PARP, or which are being actively developed, such as FEN1 [33,38,45,46]. Neither ERCC1 nor XPF knockout mice are embryonic lethal [43,47]. In contrast, knockout of both PARP1 and PARP2 genes is embryonic lethal [48], as is knockout of FEN1 [49] and this has not halted the development of inhibitors. We consider that the perceived toxicity of an ERCC1–XPF inhibitor should not constrain future development. Particularly, since recent reports suggest important additional benefits of such inhibitors: ERCC1 deficiency in combination with Olaparib enhances sensitivity to the Topoisomerase I inhibitor Camptothecin [50]; PARP inhibitors are effective against ERCC1-deficient non-small cell lung cancer cells [51].

In conclusion, in the most complete report on ERCC1–XPF inhibitors to date, we have used a combination of *in silico* and high throughput screening to identify inhibitors against the two key targets on ERCC1–XPF, the interaction domain for heterodimerization and the active site itself. Previous reports have described inhibition of the interaction between ERCC1 and XPF (however, the compounds concerned appear to be non-specific frequent hitters), or ERCC1 and XPA (unlike the ERCC1–XPF interaction, the interaction with XPA is not essential for all repair functions of ERCC1–XPF). We have identified the first active site inhibitors for ERCC1–XPF and have characterised both active site and interaction inhibitors through a fuller series of biochemical, biophysical and cancer cell-based assays than have been used previously. We have demonstrated binding to target for both interaction and active site inhibitors and shown that some of these compounds have low micromolar potency for ERCC1–XPF and display specificity in *in vitro* biochemical assays for ERCC1–XPF over two other endonucleases, including the related structure-specific endonuclease FEN1. Compounds from both inhibitor classes block Nucleotide Excision Repair in a novel assay that we developed to be suitable for automation and also sensitise melanoma cells to cisplatin. Furthermore, the best two active site inhibitors are also active in a second more conventional NER assay and show the specificity of action expected of *bona fide* ERCC1–XPF inhibitors in NER-proficient and -deficient human and mouse cells.

Conflict of interest

The authors have no conflicts of interest to declare.

Funding source

EMM was supported by a Ph.D. Scholarship from Cancer Research UK. This work was supported by MRC Technology Development Gap Fund award A853-0118 and the University of Edinburgh.

Acknowledgements

DWM is grateful to Rick Wood (University of Texas MD Anderson at Smithville) for provision of the ERCC41 plasmid and to Alan Lehmann (Genome Damage and Stability Centre, University of Sussex) for the XP12RO cell line.

Appendix A. Supplementary data

Supplementary data associated with this article can be found, in the online version, at http://dx.doi.org/10.1016/j.dnarep.2015.04.002

References

[1] CancerStats, Cancer Research UK, 2015. http://www.cancerresearchuk.org/cancer-info/cancerstats/
[2] J.B. Korman, D.E. Fisher, Developing melanoma therapeutics: overview and update, Wiley Interdiscip. Rev. Syst. Biol. Med. 5 (2013) 257–271, http://dx.doi.org/10.1002/wsbm.1210
[3] E.M. McNeil, D.W. Melton, DNA repair endonuclease ERCC1–XPF as a novel therapeutic target to overcome chemoresistance in cancer therapy, Nucleic Acids Res. 40 (2012) 9990–10004, http://dx.doi.org/10.1093/nar/gks818
[4] G.R. Simon, S. Sharma, A. Cantor, P. Smith, G. Bepler, ERCC1 expression is a predictor of survival in resected patients with non-small cell lung cancer, Chest 127 (2005) 978–983, http://dx.doi.org/10.1378/chest.127.3.978
[5] K.A. Olaussen, A. Dunant, P. Fouret, E. Brambilla, F. André, V. Haddad, et al., DNA repair by ERCC1 in non-small-cell lung cancer and cisplatin-based adjuvant chemotherapy, N. Engl. J. Med. 355 (2006) 983–991, http://dx.doi.org/10.1056/NEJMoa060570
[6] L. Wang, J. Wei, X. Qian, H. Yin, Y. Zhao, L. Yu, et al., ERCC1 and BRCA1 mRNA expression levels in metastatic malignant effusions is associated with chemosensitivity to cisplatin and/or docetaxel, BMC Cancer 8 (2008) 97, http://dx.doi.org/10.1186/1471-2407-8-97
[7] Z. Bai, Y. Wang, H. Zhe, J. He, P. Hai, ERCC1 mRNA levels can predict the response to cisplatin-based concurrent chemoradiotherapy of locally advanced cervical squamous cell carcinoma, Radiat. Oncol. Lond. Engl. 7 (2012) 221, http://dx.doi.org/10.1186/1748-717X-7-221
[8] J.E. Bauman, M.C. Austin, R. Schmidt, B.F. Kurland, A. Vaezi, D.N. Hayes, et al., ERCC1 is a prognostic biomarker in locally advanced head and neck cancer: results from a randomised, phase II trial, Br. J. Cancer 109 (2013) 2096–2105, http://dx.doi.org/10.1038/bjc.2013.576
[9] J.A. Deloia, N.R. Bhagwat, K.M. Darcy, M. Strange, C. Tian, K. Nuttall, et al., Comparison of ERCC1/XPF genetic variation, mRNA and protein levels in women with advanced stage ovarian cancer treated with intraperitoneal platinum, Gynecol. Oncol. 126 (2012) 448–454, http://dx.doi.org/10.1016/j.ygyno.2012.05.006
[10] S. Usanova, A. Piée-Staffa, U. Sied, J. Thomale, A. Schneider, B. Kaina, et al., Cisplatin sensitivity of testis tumour cells is due to deficiency in interstrand-crosslink repair and low ERCC1–XPF expression, Mol. Cancer 9 (2010) 248, http://dx.doi.org/10.1186/1476-4598-9-248
[11] M. Selvakumaran, D.A. Pisarcik, R. Bao, A.T. Yeung, T.C. Hamilton, Enhanced cisplatin cytotoxicity by disturbing the nucleotide excision repair pathway in ovarian cancer cell lines, Cancer Res. 63 (2003) 1311–1316, PubMed PMID: 12649192.
[12] S. Arora, A. Kothandapani, K. Tillison, V. Kalman-Maltese, S.M. Patrick, Down-regulation of XPF-ERCC1 enhances cisplatin efficacy in cancer cells, DNA Repair 9 (2010) 745–753, http://dx.doi.org/10.1016/j.dnarep.2010.03.010
[13] I.-Y. Chang, M.-H. Kim, H.B. Kim, D.Y. Lee, S.-H. Kim, H.-Y. Kim, et al., Small interfering RNA-induced suppression of ERCC1 enhances sensitivity of human cancer cells to cisplatin, Biochem. Biophys. Res. Commun. 327 (2005) 225–233, http://dx.doi.org/10.1016/j.bbrc.2004.12.008
[14] L. Song, A.-M. Ritchie, E.M. McNeil, W. Li, D.W. Melton, Identification of DNA repair gene Ercc1 as a novel target in melanoma, Pigment Cell Melanoma Res. 24 (2011) 966–971, http://dx.doi.org/10.1111/j.1755-148X.2011.00882.x
[15] O.V. Tsodikov, J.H. Enzlin, O.D. Schärer, T. Ellenberger, Crystal structure and DNA binding functions of ERCC1, a subunit of the DNA structure-specific endonuclease XPF-ERCC1, Proc. Natl. Acad. Sci. U. S. A. 102 (2005) 11236–11241, http://dx.doi.org/10.1073/pnas.0504341102
[16] O.V. Tsodikov, D. Ivanov, B. Orelli, L. Staresincic, I. Shoshani, R. Oberman, et al., Structural basis for the recruitment of ERCC1–XPF to nucleotide excision repair complexes by XPA, EMBO J. 26 (2007) 4768–4776, http://dx.doi.org/10.1038/sj.emboj.7601894
[17] K. Tripsianes, G. Folkers, E. Ab, D. Das, H. Odijk, N.G.J. Jaspers, et al., The structure of the human ERCC1/XPF interaction domains reveals a complementary role for the two proteins in nucleotide excision repair, Struct. Lond. Engl. 1993 13 (2005) 1849–1858, http://dx.doi.org/10.1016/j.str.2005.08.014
[18] Y.-J. Choi, K.-S. Ryu, Y.-M. Ko, Y.-K. Chae, J.G. Pelton, D.E. Wemmer, et al., Biophysical characterization of the interaction domains and mapping of the contact residues in the XPF–ERCC1 complex, J. Biol. Chem. 280 (2005) 28644–28652, http://dx.doi.org/10.1074/jbc.M501083200
[19] P.H. Gaillard, R.D. Wood, Activity of individual ERCC1 and XPF subunits in DNA nucleotide excision repair, Nucleic Acids Res. 29 (2001) 872–879, PubMed PMID: 11160918.
[20] J. Sgouros, P.H. Gaillard, R.D. Wood, A relationship between a DNA-repair/recombination nuclease family and archaeal helicases, Trends Biochem. Sci. 24 (1999) 95–97, PubMed PMID: 10203755.
[21] T. Nishino, K. Komori, D. Tsuchiya, Y. Ishino, K. Morikawa, Crystal structure and functional implications of *Pyrococcus furiosus* hef helicase domain involved in branched DNA processing, Struct. Lond. Engl. 1993 13 (2005) 143–153, http://dx.doi.org/10.1016/j.str.2004.11.008

[22] J.H. Enzlin, O.D. Schärer, The active site of the DNA repair endonuclease XPF-ERCC1 forms a highly conserved nuclease motif, EMBO J. 21 (2002) 2045–2053, http://dx.doi.org/10.1093/emboj/21.8.2045
[23] H. Jiang, L.Y. Yang, Cell cycle checkpoint abrogator UCN-01 inhibits DNA repair: association with attenuation of the interaction of XPA and ERCC1 nucleotide excision repair proteins, Cancer Res. 59 (1999) 4529–4534, PubMed PMID: 10493501.
[24] K.H. Barakat, J. Torin Huzil, T. Luchko, L. Jordheim, C. Dumontet, J. Tuszynski, Characterization of an inhibitory dynamic pharmacophore for the ERCC1-XPA interaction using a combined molecular dynamics and virtual screening approach, J. Mol. Graph. Model. 28 (2009) 113–130, http://dx.doi.org/10.1016/j.jmgm.2009.04.009
[25] K.H. Barakat, L.P. Jordheim, R. Perez-Pineiro, D. Wishart, C. Dumontet, J.A. Tuszynski, Virtual screening and biological evaluation of inhibitors targeting the XPA–ERCC1 interaction, PLoS ONE 7 (2012) e51329, http://dx.doi.org/10.1371/journal.pone.0051329
[26] L.P. Jordheim, K.H. Barakat, L. Heinrich-Balard, E.-L. Matera, E. Cros-Perrial, K. Bouledrak, et al., Small molecule inhibitors of ERCC1–XPF protein–protein interaction synergize alkylating agents in cancer cells, Mol. Pharmacol. 84 (2013) 12–24, http://dx.doi.org/10.1124/mol.112.082347
[27] I. Kuraoka, W.R. Kobertz, R.R. Ariza, M. Biggerstaff, J.M. Essigmann, R.D. Wood, Repair of an interstrand DNA cross-link initiated by ERCC1–XPF repair/recombination nuclease, J. Biol. Chem. 275 (2000) 26632–26636, http://dx.doi.org/10.1074/jbc.C000337200
[28] M. Bowles, J. Lally, A.J. Fadden, S. Mouilleron, T. Hammonds, N.Q. McDonald, Fluorescence-based incision assay for human XPF-ERCC1 activity identifies important elements of DNA junction recognition, Nucleic Acids Res. 40 (2012) e101, http://dx.doi.org/10.1093/nar/gks284
[29] M.A. Wear, A. Patterson, K. Malone, C. Dunsmore, N.J. Turner, M.D. Walkinshaw, A surface plasmon resonance-based assay for small molecule inhibitors of human cyclophilin A, Anal. Biochem. 345 (2005) 214–226, http://dx.doi.org/10.1016/j.ab.2005.06.037
[30] W.L. de Laat, E. Appeldoorn, N.G. Jaspers, J.H. Hoeijmakers, DNA structural elements required for ERCC1–XPF endonuclease activity, J. Biol. Chem. 273 (1998) 7835–7842, PubMed PMID: 9525876.
[31] U. Ghosh, K. Giri, N.P. Bhattacharyya, Interaction of aurintricarboxylic acid (ATA) with four nucleic acid binding proteins DNase I, RNase A, reverse transcriptase and Taq polymerase, Spectrochim. Acta. A: Mol. Biomol. Spectrosc. 74 (2009) 1145–1151, http://dx.doi.org/10.1016/j.saa.2009.09.024
[32] R.B. Hallick, B.K. Chelm, P.W. Gray, E.M. Orozco Jr., Use of aurintricarboxylic acid as an inhibitor of nucleases during nucleic acid isolation, Nucleic Acids Res. 4 (1977) 3055–3064, PubMed PMID: 410006.
[33] D. Dorjsuren, D. Kim, D.J. Maloney, D.M. Wilson, A. Simeonov, Complementary non-radioactive assays for investigation of human flap endonuclease 1 activity, Nucleic Acids Res. 39 (2011) e11, http://dx.doi.org/10.1093/nar/gkq1082
[34] M. Newman, J. Murray-Rust, J. Lally, J. Rudolf, A. Fadden, P.P. Knowles, et al., Structure of an XPF endonuclease with and without DNA suggests a model for substrate recognition, EMBO J. 24 (2005) 895–905, http://dx.doi.org/10.1038/sj.emboj.7600581
[35] L.A. Kelley, M.J.E. Sternberg, Protein structure prediction on the Web: a case study using the Phyre server, Nat. Protoc. 4 (2009) 363–371, http://dx.doi.org/10.1038/nprot.2009.2
[36] J.H. Zhang, T.D. Chung, K.R. Oldenburg, A simple statistical parameter for use in evaluation and validation of high throughput screening assays, J. Biomol. Screen. 4 (1999) 67–73, PubMed PMID: 10838414.
[37] M. Habig, A. Blechschmidt, S. Dressler, B. Hess, V. Patel, A. Billich, et al., Efficient elimination of nonstoichiometric enzyme inhibitors from HTS hit lists, J. Biomol. Screen. 14 (2009) 679–689, http://dx.doi.org/10.1177/1087057109336586
[38] L.N. Tumey, D. Bom, B. Huck, E. Gleason, J. Wang, D. Silver, et al., The identification and optimization of a N-hydroxy urea series of flap endonuclease 1 inhibitors, Bioorg. Med. Chem. Lett. 15 (2005) 277–281, http://dx.doi.org/10.1016/j.bmcl.2004.10.086
[39] M. Biggerstaff, D.E. Szymkowski, R.D. Wood, Co-correction of the ERCC1, ERCC4 and xeroderma pigmentosum group F DNA repair defects in vitro, EMBO J. 12 (1993) 3685–3692, PubMed PMID: 8253090.
[40] Y. Wang, J. Xiao, T.O. Suzek, J. Zhang, J. Wang, Z. Zhou, et al., PubChem's BioAssay database, Nucleic Acids Res. 40 (2012) D400–D412, http://dx.doi.org/10.1093/nar/gkr1132
[41] A.M. Sijbers, P.J. van der Spek, H. Odijk, J. van den Berg, M. van Duin, A. Westerveld, et al., Mutational analysis of the human nucleotide excision repair gene ERCC1, Nucleic Acids Res. 24 (1996) 3370–3380, PubMed PMID: 8811092.
[42] W.L. de Laat, A.M. Sijbers, H. Odijk, N.G. Jaspers, J.H. Hoeijmakers, Mapping of interaction domains between human repair proteins ERCC1 and XPF, Nucleic Acids Res. 26 (1998) 4146–4152, PubMed PMID: 9722633.
[43] J. McWhir, J. Selfridge, D.J. Harrison, S. Squires, D.W. Melton, Mice with DNA repair gene (ERCC-1) deficiency have elevated levels of p53, liver nuclear abnormalities and die before weaning, Nat. Genet. 5 (1993) 217–224, http://dx.doi.org/10.1038/ng1193-217
[44] G. Weeda, I. Donker, J. de Wit, H. Morreau, R. Janssens, C.J. Vissers, et al., Disruption of mouse ERCC1 results in a novel repair syndrome with growth failure, nuclear abnormalities and senescence, Curr. Biol. 7 (1997) 427–439, PubMed PMID: 9197240.
[45] C. McWhirter, M. Tonge, H. Plant, I. Hardern, W. Nissink, S.T. Durant, Development of a high-throughput fluorescence polarization DNA cleavage assay for the identification of FEN1 inhibitors, J. Biomol. Screen. 18 (2013) 567–575, http://dx.doi.org/10.1177/1087057113476551
[46] L.N. Tumey, B. Huck, E. Gleason, J. Wang, D. Silver, K. Brunden, et al., The identification and optimization of 2,4-diketobutyric acids as flap endonuclease 1 inhibitors, Bioorg, Med. Chem. Lett. 14 (2004) 4915–4918, http://dx.doi.org/10.1016/j.bmcl.2004.07.028
[47] M. Tian, R. Shinkura, N. Shinkura, F.W. Alt, Growth retardation, early death, and DNA repair defects in mice deficient for the nucleotide excision repair enzyme XPF, Mol. Cell. Biol. 24 (2004) 1200–1205, PubMed PMID: 14729965.
[48] J. Ménissier de Murcia, M. Ricoul, L. Tartier, C. Niedergang, A. Huber, F. Dantzer, et al., Functional interaction between PARP-1 and PARP-2 in chromosome stability and embryonic development in mouse, EMBO J. 22 (2003) 2255–2263, http://dx.doi.org/10.1093/emboj/cdg206
[49] E. Larsen, C. Gran, B.E. Saether, E. Seeberg, A. Klungland, Proliferation failure and gamma radiation sensitivity of Fen1 null mutant mice at the blastocyst stage, Mol. Cell. Biol. 23 (2003) 5346–5353, http://dx.doi.org/10.1128/MCB.23.15.5346-5353.2003
[50] Y.-W. Zhang, M. Regairaz, J.A. Seiler, K.K. Agama, J.H. Doroshow, Y. Pommier, Poly(ADP-ribose) polymerase and XPF-ERCC1 participate in distinct pathways for the repair of topoisomerase I-induced DNA damage in mammalian cells, Nucleic Acids Res. 39 (2011) 3607–3620, http://dx.doi.org/10.1093/nar/gkq1304
[51] S. Postel-Vinay, I. Bajrami, L. Friboulet, R. Elliott, Y. Fontebasso, N. Dorvault, et al., A high-throughput screen identifies PARP1/2 inhibitors as a potential therapy for ERCC1-deficient non-small cell lung cancer, Oncogene 32 (2013) 5377–5387, http://dx.doi.org/10.1038/onc.2013.311.